Materials Transactions, Vol. 53, No. 4 (2012) pp. 627 to 630
Special Issue on APCNDT 2009

Numerical Analysis of Microwave NDT Applied to Piping Inspection

Yasutomo Sakai*, Noritaka Yusa, Satoshi Ito and Hidetoshi Hashizume

Department of Quantum Science and Energy Engineering, School of Engineering, Tohoku University, Sendai 980-8579, Japan

Numerical simulations using finite element software were carried out to discuss the physical background of nondestructive inspections of pipes using microwaves. The simulations were conducted using an axisymmetric configuration modeling pipe with wall thinning to evaluate the effect of the profile of the wall thinning on the microwave propagation. Both rectangular and quasi-racetrack wall thinnings were considered. The numerical simulations showed the presence of wall thinning attenuates microwaves at particular frequencies. An empirical formula was proposed to evaluate the profile of wall thinning for the particular frequencies. Although the formula was based on the results of numerical simulations considering only rectangular wall thinning, it is also applicable to the evaluation of quasi-racetrack wall thinning.
[doi:10.2320/matertrans.I-M2012805]

(Received November 12, 2009; Accepted March 11, 2011; Published February 29, 2012)

Keywords: *microwave, piping, finite element method, electro-magnetic NDT, wall thinning*

1. Introduction

Rapid and reliable non-destructive inspections of piping systems play an important role in the maintenance of large structures such as power and chemical plants. Whereas several conventional non-destructive testing methods including eddy current and ultrasonic testing are used for the inspection of piping systems, these conventional methods can only detect defects existing in the vicinity of the probe. Consequently, these methods require scanning probes along the piping, leading to a long inspection period when a piping system is large and complicated. Novel non-destructive testing methods that can inspect long piping systems simultaneously are in high demand for more efficient maintenance.

Recent studies have reported the application of guided waves in the inspection of piping systems. The guided wave propagates in the axial direction of the piping, which enables the pipe to be evaluated from the reflected/refracted waves. Studies have reported success in evaluating notches from these guided wave signals both by simulations and experiments.[1)] More recent studies have demonstrated the effectiveness of signal processing[2)] and imaging methods[3)] in nondestructive testing signals obtained using guided wave inspections. In contrast, one of the disadvantages of the guided wave method in practical usage is that it needs physical contact between the transducers and the piping. Furthermore, in general, the contact force significantly affects the signals obtained.

On the basis of the background above, several studies have proposed the application of microwaves.[4–7)] Unlike microwave nondestructive testing using near-field techniques,[8)] the key idea is to regard a pipe as a waveguide. The microwaves are propagated inside a pipe and the integrity of approximate size and location of defect in the pipe is evaluated from the reflection and transmission of the microwaves. While the principle is similar to those using wave guides, the inspection using microwaves does not require physical contact between the probe and the pipes to be inspected. Earlier studies have demonstrated that wall thinning, artificially fabricated into a pipe, disturb the propagation of microwaves and it is possible to detect the defect.[5,7)] Furthermore, they also revealed that the time of flight (TOF) of reflected microwave enables microwave testing to locate a defect as well as the end of a pipe. The results obtained are in good agreement with theoretical results. However, the quantitative relationship between defect profiles and signals, as well as the behavior of microwaves near defects, remains unclear. This study, therefore, aims to establish this relationship under an assumption that the location of a defect and the length of a pipe are known in advance.

2. Materials and Methods

This study evaluates the propagation of microwaves inside a circular pipe using finite element simulations. The configuration of the numerical simulations is illustrated in Fig. 1. The simulations were carried out using an axisymmetric configuration modeling of a pipe with full circumferential wall thinning at its center. Two wall thinning profiles were considered in this study. One was with a rectangular cross-sectional profile with a depth of D and an axial length of W, and the other was with a quasi-racetrack one with a depth of D, a total axial length of W, and an axial length of the straight region of L. Dimensions considered in the simulations are summarized in Table 1. The inner radius of the pipe was 29.75 mm, which gave the lowest cut-off frequency of 3.8 GHz when there was no wall thinning. The length of a pipe was set to 200 mm.

In the numerical simulations, Port 1 generated a microwave of TM_{01} mode at a given frequency, f, and Port 2 provided no reflection. The frequencies considered in this study ranged from 4 to 15 GHz. The inner surfaces of the pipe were modeled as a perfect conductor and inside of the pipe was filled with air whose conductivity, relative permeability, and relative permittivity are 0 [S/m], 1, and 1, respectively. The numerical simulations were carried out using a finite element software, COMSOL Multiphysics together with its RF module, and solved the Maxwell

*Graduate Student, Tohoku University. Present address: Nippon Kaiji Kyoukai, Tokyo 102-8567, Japan

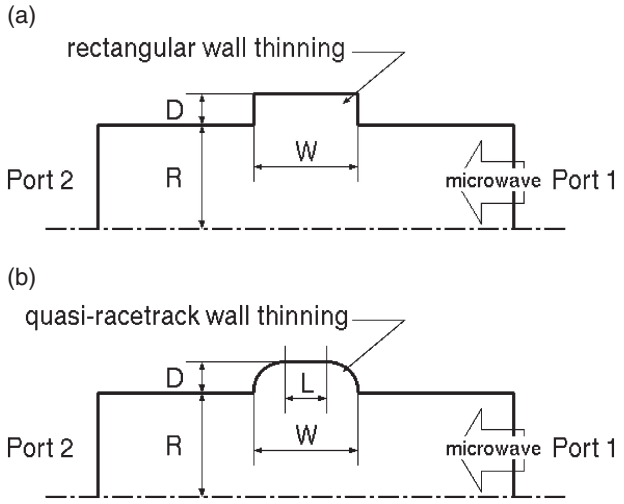

Fig. 1 Numerical configuration. (a) Rectangular wall thinning model (b) Quasi-racetrack wall thinning model.

Table 1 Parameter of wall thinning.

	Rectangular	Quasi-racetrack
D [mm]	0, 0.5, 1, 2, 3, 4	1, 2, 3, 4
W [mm]	20, 30, 40, 50, 60	40
L [mm]	$= W$	0, 10, 30

equations as a time-harmonic problem in a two-dimensional axisymmetric configuration. Approximately 160,000 quadratic triangle edge elements were employed. The minimum and maximum sizes of the elements were 0.5 and 1.2 mm.

3. Results and Discussion

Figure 2 shows the dependency of the voltage transmission coefficient from Port 1 to Port 2, S_{21}. When there is no defect, the microwave barely attenuates at all and thus S_{21} remains 0 dB (results not shown). In contrast, the presence of wall thinning significantly attenuates the microwave propagations at several specific frequencies that are not identical but close to resonant frequencies. These frequencies can be calculated if the pipe with a wall thinning is regarded as a resonant cavity. Figure 2(a) presents dependencies of two rectangular wall thinnings with the same axial length of 40 mm and different depths of 2 and 4 mm. The figure shows that there are two groups. One is near 9 GHz and the other is near 13 GHz; the former and the latter are termed as group a and b, respectively, for purposes of illustration. Three clear negative peaks contained in each group are numbered in order of their frequency, as f_{X1}, f_{X2}, f_{X3}, where X indicates the group the peak belongs to. In general, these frequencies become smaller when the defect is deeper. Figure 2(b) shows how the cross-sectional profile affects the dependency, which indicates that the frequencies of the negative peaks do not depend on the cross-sectional profile so significantly. It should be noted here that in the numerical simulations frequencies were changed with a pitch of almost 0.05 GHz. Thus, it is not always accurate to compare the minimum values of S_{21} especially those at sharp points.

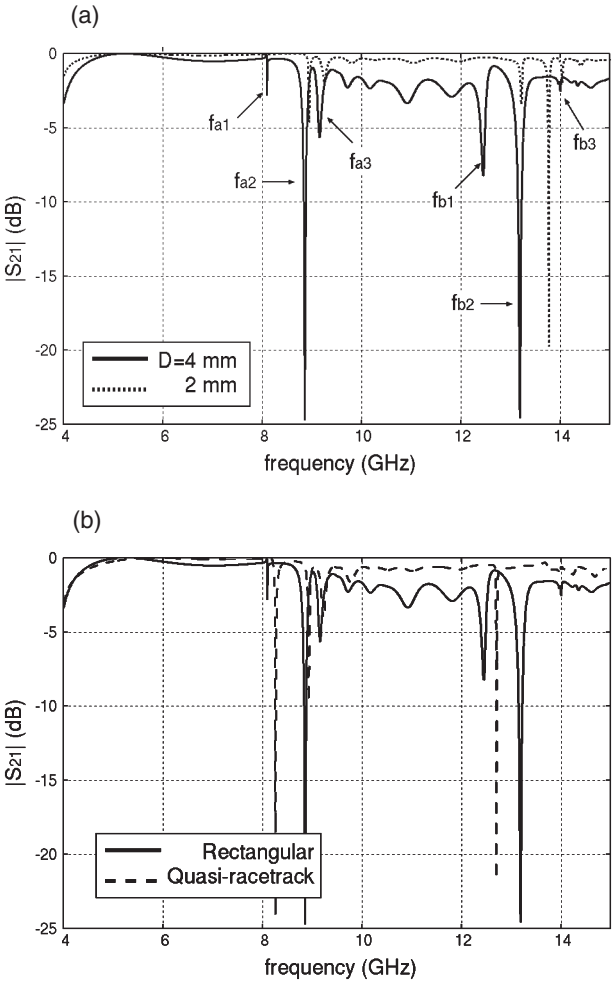

Fig. 2 Dependency of the magnitude of S_{21} on frequency. (a) Two rectangular wall thinnings, $W = 40$ mm, $D = 2$ and 4 mm. (b) Rectangular wall thinning of $W = 40$ and $D = 4$ mm, and quasi-racetrack wall thinning of $W = 40$, $D = 4$, and $L = 0$ mm.

Fig. 3 Distributions of magnetic field inside pipe (left: no wall thinning, center: rectangular wall thinning of $W = 40$ and $D = 4$ mm, right: quasi-racetrack wall thinning of $W = 40$, $D = 4$, and $L = 0$ mm). (a) $f = 6$ GHz (b) $f = 8.836$ GHz (left and center) and 8.930 GHz (right) (c) $f = 10$ GHz (d) $f = 12.36$ GHz (left and center) and 12.65 GHz (right).

Figure 3 presents the distribution of magnetic fields at several frequencies. The figure shows that when there is no wall thinning, microwaves of the TM_{01} mode with a clear periodicity are generated regardless of frequency. When there is wall thinning, however, the periodicity is disturbed

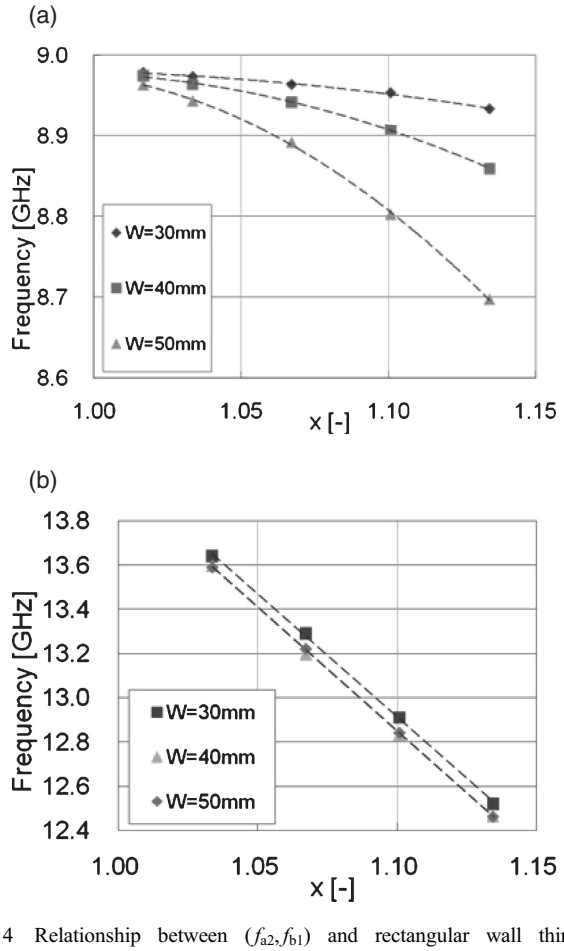

Fig. 4 Relationship between (f_{a2},f_{b1}) and rectangular wall thinning profiles. (a) f_{a2} (b) f_{b1}.

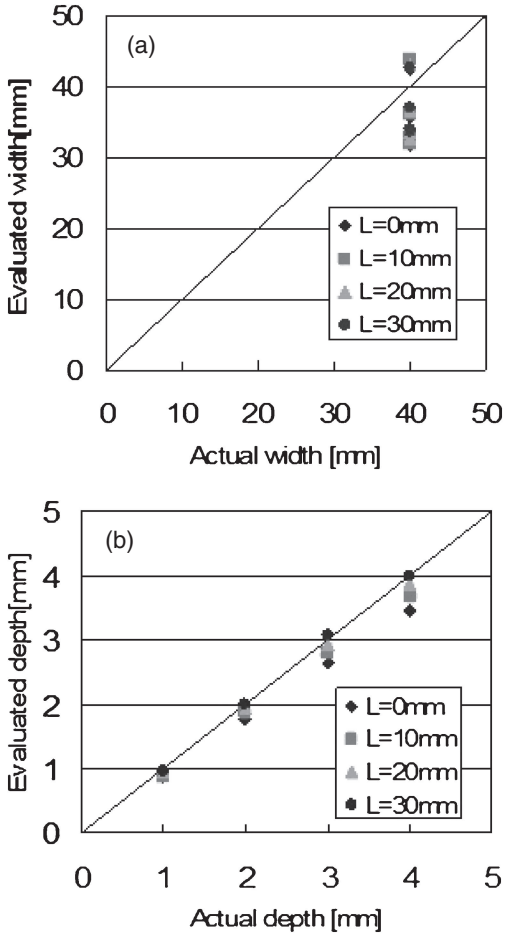

Fig. 5 Evaluated and actual profiles of quasi-racetrack wall thinnings. (a) axial length (b) depth.

significantly especially when the frequency is close to the negative peaks, and only a part of the microwave reaches Port 2. The distribution of the magnetic fields near the wall thinning shows that negative peaks contained in group a and b stem from TM_{02} and TM_{03} modes, respectively.

We now attempt to evaluate the profile of wall thinning from the frequencies. Since at times it was difficult to confirm f_{a1}, f_{a3}, f_{b2}, and f_{b3}, the frequencies denoted as f_{a2} and f_{b1} are used. Figure 4 shows relationship between these two frequencies and the profile of wall thinning. Analyzing the data gave a polynomial approximation of:

$$f_{a2} = (-0.498W + 13.91)x^2 + (0.9787W - 27.95)x + (-0.4837W + 23.16) \quad (1)$$

and

$$f_{b1} = -0.00275W - 11.13x + 25.22 \quad (2)$$

where x is the normalized wall thinning depth defined as $x = (R + D)/R$, where R is the radius of the pipes. These indicate the possibility of evaluating the axial length and the depth of a wall thinning from the frequencies. The results of evaluating the quasi-racetrack wall thinnings using these equations are given in Fig. 5. Although the equations are based only on the results of the wall thinnings of rectangular cross-sections, the results indicate that it is possible to evaluate the depth of quasi-racetrack wall thinning from the equations quite accurately, whereas a wall thinning with a smooth boundary profile tends to be evaluated to a shallower level. Figure 5(a) shows that the error in evaluating the width of a wall thinning is as much as 10 mm. Further investigation revealed that the plausible reason for that is that the L of such shallow defect does not have large influence on f_{a2} whereas it affects f_{b1} significantly.

This study assumed that the location of wall thinning and the length of pipes are known in advance. Whereas considering other configuration requires different equations, the equations can be easily obtained based on numerical simulations.

4. Conclusions

The propagation of microwaves inside pipes with wall thinning was analyzed using numerical analysis to discuss the applicability of microwave nondestructive testing to pipe inspection. The presence of a wall thinning attenuates the microwave and S_{21} drops at several specific frequencies. The relationship between the frequency and the profile of wall thinning was analyzed from the results of the numerical simulations. An empirical formula was proposed to evaluate the cross-sectional profile of wall thinning from frequencies that give a negative peak of S_{21}. Although the equations were based only on the results of rectangular cross-sectional wall thinnings obtained by the numerical simulations, the results implied that a wall thinning with more a complicated

boundary profile could also be evaluated. Since an earlier study of the authors showed that it is possible to locate the position of defects in pipes using the time-of-flight of microwave signals,[5] the results obtained in this study would lead to a nondestructive testing method that can very quickly locate and evaluate defects appearing in a long pipe.

REFERENCES

1) D. N. Alleyne, M. J. S. Lowe and P. Gawley: J. Appl. Mech. **65** (1998) 635–641.
2) P. D. Wilcox: Ultrason. Ferroelectrics Frequency Control **50** (2003) 419–427.
3) T. Hayashi, M. Nagao and M. Murase: J. Japan Soc. Mech. Eng. Ser. A **72** (2006) 1941–1948 (in Japanese).
4) H. Hashizume, T. Shibara and K. Yuki: Int. J. Appl. Electromagn. Mech. **20** (2004) 171–178.
5) K. Abbasi, S. Ito and H. Hashizume: Int. J. Appl. Electromagn. Mech. **28** (2008) 429–439.
6) Y. Ju, L. Liu and M. Ishikawa: Mater. Sci. Forum **614** (2009) 111–116.
7) Y. Sakai, N. Yusa and H. Hashizume: Proc. 15th Int. Workshop on Electromagnetic Nondestructive Evaluation, (2010) pp. 49–50.
8) M. Saka, Y. Ju, D. Luo and H. Abe: JSME Int. J. Ser. A **45** (2002) 573–578.